ACI STRUCTURAL JOURNAL TECHNICAL PAPER

Title no. 98-S19

Analysis of Reinforced Concrete Shells for Transverse Shear and Torsion

by Taira Yamamoto and Frank J. Vecchio

Finite element formulations are presented for improved analysis of reinforced concrete shell structures critical in shear. The nonlinear methodology developed, based on the use of layered isoparametric finite elements, allows for explicit consideration of out-of-plane shear deformations. Cracked concrete is treated as an orthotropic nonlinear material in the context of smeared rotating cracks, and the tension softening model implemented uses a consistent average stress-strain approach based on fracture energy.

The accuracy of the formulation is examined by investigating three different series of test specimens: simple beams, with and without shear reinforcement, subjected to transverse shear and flexure; hollow rectangular over- and under-reinforced beams subjected to torsion and flexure; and a scale model of an offshore structure subjected to hydrostatic pressure. Good agreement between predicted and observed response was found for all series of tests examined.

Keywords: reinforced concrete; shear; tension; test.

INTRODUCTION

Large and highly complex reinforced concrete shell structures, such as offshore structures, have been built with increasing regularity in recent years. Although typically analyzed as thin-wall shells in the early design stages, the actual thickness of the structural elements involved is often quite large. In such thick-shell structures, the effects of out-of-plane shear behavior is frequently a critical design issue and must be expressly addressed. Indeed, many designs incorporate substantial amounts of out-of-plane reinforcement; reinforcement that is considerably more expensive and difficult to place than in-plane reinforcement (Fig. 1). In applying advanced procedures to the analysis of such structures, it is thus necessary to incorporate transverse shear behavior into the analysis algorithm.

Over the last 30 years, a variety of procedures have been reported in the literature for analysis of concrete shells (Jofriet and McNiece 1971; Hand, Pecknold, and Schnobrich 1977; Scordelis and Chan 1987; Hu and Schnobrich 1991; and Di and Cheung 1993). The majority of these formulations have concentrated on modeling aspects of behavior associated with flexural mechanisms. Only recently have researchers become concerned with addressing problems associated with transverse shear effects, with notable contributions made by Cervera, Hinton, and Hassan (1987), Harmon and Zhangyuan (1989), and Polak (1998).

A nonlinear finite element shell analysis program for reinforced concrete shells was previously developed (Polak and Vecchio 1993). The program adopts a layered shell formulation that specifically includes provisions for out-of-plane shear behavior, and incorporates the constitutive models of the modified compression field theory (MCFT) (Vecchio and Collins 1986). While the program was fully corroborated for various types of element-level behavior, primarily involving panel or slab type structures, it was not extensively tested for structure-level behavior. In particular, the accuracy in modeling behavior in shear-critical thick-wall shell structures has not been fully verified.

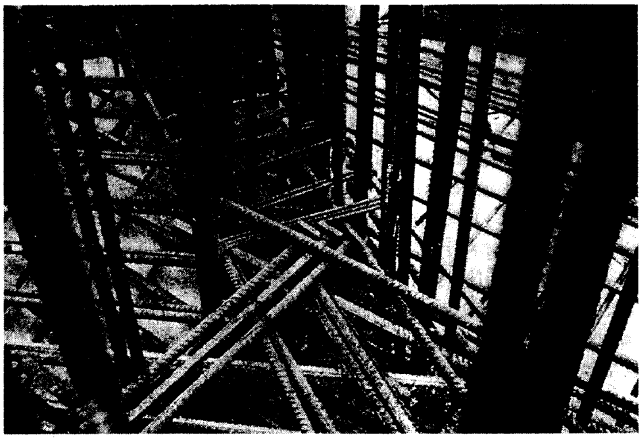

Fig. 1—Placement of shear reinforcement in tricell wall of offshore structure.

The work described herein is aimed at improving and corroborating nonlinear analysis procedures for reinforced concrete shell structures that are significantly influenced by shear. Specific objectives are: 1) to develop an appropriate concrete tension model that can be incorporated into the finite element shell formulation, consistent with the theoretical approach of the MCFT; 2) to corroborate the tension model and analysis procedure for structural elements critical in out-of-plane shear; 3) to verify accuracy in problems involving torsional stresses and/or in-plane shear; and 4) to investigate behavior and modeling accuracy in situations involving complex three-dimensional and indeterminate actions.

RESEARCH SIGNIFICANCE

The design and behavior of a large reinforced concrete shell structure is frequently influenced by aspects associated with out-of-plane shear or torsion. Improper consideration of these shear mechanisms can result in inadequately reinforced and potentially unsafe structures, or conversely in an unnecessary provision of excessive amounts of expensive transverse reinforcement. Currently, many of the analytical procedures available are inadequate in this regard. The formulations

ACI Structural Journal, V. 98, No. 2, March-April 2001.
MS No. 00-096 received April 18, 2000 and reviewed under Institute publication policies. Pertinent discussion will be published in the January-February 2002 *ACI Structural Journal* if received by September 1, 2001.

Taira Yamamoto *is a design engineer with the Underground Storage Facility Design Section, Civil Engineering Division, of the Taisei Corp. of Japan. He recently completed a MASc degree in the Civil Engineering Department, University of Toronto.*

ACI member **Frank J. Vecchio** *is Professor and Associate Chair in the Department of Civil Engineering, University of Toronto. He is Deputy Chair of* fib *Commission 4 (Modeling of Structural Behavior and Design), Chair of* fib *Task Group 4.4 (Computer-Based Methods), and a member of Joint ACI-ASCE Committee 447, Finite Element Analysis of Reinforced Concrete Structures (FEARC). His research interests include nonlinear analysis and design of concrete structures, constitutive modeling, assessment, and repair and rehabilitation of structures.*

presented herein will contribute to more rational and accurate analyses of shear-related problems in concrete shell structures.

FINITE ELEMENT FORMULATION

The basis for the model formulations and analytical studies described herein is a nonlinear finite element analysis (NLFEA) program for reinforced concrete shells described previously by Polak and Vecchio (1993) and recently refined: program VecTor4. One of the principal features of the program formulation adopted is the consideration of transverse shear deformations, based on the assumption of a constant normal shear strain through the thickness of the shell element. The formulation is also based on other typical assumptions used in Mindlin plate theory; that is: 1) normals to the midsurface remain straight but not necessarily normal after deformation; and 2) resultant stresses normal to the midsurface are negligible.

Degenerated quadratic isoparametric shell elements are employed in the algorithm developed; specifically, a nine-noded 42 degree-of-freedom Heterosis element is favored. Quadratic shape functions are used to describe element geometry, allowing it to have curved sides and a curved surface. All side and corner nodes have three translational and two rotational degrees of freedom; the central ninth node has only the two rotational degrees of freedom. A principal advantage of the Heterosis element is that it exhibits good behavior for both thick and thin shells.

To determine the element stiffness matrix, numerical integration over the volume is required. For the case of a quadratic shell element, the 3 x 3 rule is the desired order of gauss quadrature since an element evaluated accordingly will generally not exhibit numerical difficulties and comply with convergence criteria. However, especially when thin elements are used, shear locking may occur. The use of the reduced 2 x 2 integration rule to evaluate the shear stiffness is an effective remedy to shear locking. Hence, selective integration is used; the 3 x 3 rule is used for evaluating the bending stiffness components and the 2 x 2 rule is used for the shear stiffness components. When using the reduced integration rule, problems with zero energy modes may arise. With the Heterosis element, however, only one zero energy mode exists, and it is not communicable when more than one element is used.

Since reinforced concrete exhibits highly nonlinear material behavior, an appropriate integration scheme through the thickness must be employed. In VecTor4, a layered shell formulation is used. Up to 16 layers are used to model the shell thickness, where each layer has the same thickness and concrete properties. Steel layers are superimposed to model the in-plane reinforcement. The location of the steel layers is established by specifying the distance of the centroid of the reinforcement relative to the top surface of the element. Out-of-plane (transverse shear) reinforcement is treated as smeared and defined as a property of the concrete layers.

The solution algorithm used in the NLFEA formulation is a full-load, direct iteration procedure based on variable secant moduli. The solution algorithm accommodates both nonlinear material and nonlinear geometric behavior. A complete description of the finite element formulation is given in Polak and Vecchio (1993).

CONSTITUTIVE MODELING

The constitutive modeling approach used in VecTor4 is based on the MCFT (Vecchio and Collins 1986). A basic assumption of this theory is that the directions of principal stress and principal strain coincide; that is, the MCFT is a smeared rotating crack model. Cracked concrete is treated as an orthotropic nonlinear elastic material based on average strains and average stresses over distances spanning several cracks. The stress-strain relationships used for the concrete in compression reflect the effects of compression softening, referring to the reduction in compressive strength and stiffness of concrete due to the influence of transverse cracking. For concrete in tension, the formulation employed models tension stiffening effects; that is, postcracking tensile stresses in concrete due to the influence of bond action with the reinforcement. These mechanisms were found to be important in describing the behavior of shear critical elements.

Although the constitutive relations of the MCFT are principally cast in terms of average strains and average stresses, attention is also paid to local stress conditions at crack surfaces. Specifically, the possibility of slip along crack surfaces due to localized shear stresses and the yielding of reinforcement across cracks is examined. These local mechanisms can be particularly important in elements containing light amounts of shear reinforcement and subjected to high shear stresses.

A full description of the constitutive models of the MCFT is given by Vecchio and Collins (1986).

Concrete tension mechanisms

In cracked reinforced concrete structures, reinforcement imparts some load (stress) to the concrete between cracks via bond action. The mechanism, commonly known as tension stiffening, is effectively responsible for above-zero average tensile stresses existing in cracked concrete. These average concrete tensile stresses act to increase the stiffness of the element, although capacity is still governed by the ability of the reinforcement to carry the entire load across the cracks.

The influence of the reinforcement is limited to a volume of concrete in relatively close proximity to the bar; this zone is termed the tension-stiffening zone (Fig. 2). According to past CEB guidelines (CEB 1990), it was assumed that the extent of influence was limited to concrete within 7.5 bar diameters from the reinforcement. Outside this zone, the second mechanism of postcracking concrete tension prevails, that of tension softening. Herein, tensile stresses are developed by the fracture process and by aggregate interlock mechanisms.

Recent developments in the application of fracture mechanics to concrete have made it possible to effectively analyze the postcracking behavior of plain concrete via the finite element method. These applications have incorporated tension-softening models to describe the gradual decay of stress (or strain softening) in plain concrete in tension as cracking propagates. Several researchers adopting a tension softening model have obtained fairly consistent results (for example,

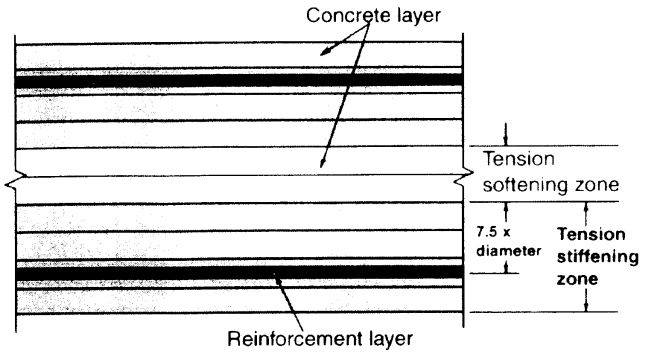

Fig. 2—Layered shell element with tension stiffening zone defined.

ASCE 1993; Mihashi et al. 1993; and An et al. 1997). Consequently, it is commonly accepted that the consideration of tension softening is indispensable in analyzing the behavior of concrete structures with relatively large unreinforced areas.

When a homogeneous plain concrete element subjected to a uniaxial load is partitioned into finite length elements, as shown in Fig. 3(a), the stress-strain relationship can be defined from the softening curve (stress versus crack-width relationship) shown in Fig. 3(b). Note that this relationship is a function of a single element length h; that is, a crack is assumed to occur in a single element. The area under the softening curve is defined as the fracture energy G_f. (Although a simple linear softening curve is shown, a variety of linear and nonlinear softening models have been proposed.) The fracture energy G_f is defined as the energy required to form a complete crack, and is usually obtained from a three-point bending test of a notched prism. The value of G_f can be estimated by the method proposed in the CEB-FIP Model Code (1990), in which G_f is a function of the compressive strength of the concrete and the maximum aggregate size. Recent research by Darwin (1999), however, indicates that G_f is relatively independent of the concrete strength or aggregate size.

The complete inclusion of a tension softening model in a nonlinear finite element analysis algorithm entails the use of sophisticated bifurcation analysis and small load increments. This adds considerably to the computational burden of the analysis. In addition, it is difficult to formulate the crack localization in a layered shell element because, when a transverse shear crack is considered, the crack localization must be considered across several layers in an element. Since a main advantage of the layered shell formulation is that the stiffness calculation of each layer is independent from the adjacent layers, the crack localization approach will render the finite element formulation significantly more complicated. To overcome these difficulties and make possible the implementation of a tension-softening model in finite element shell analysis, an average stress-strain approach is envisaged. A model formulated accordingly follows.

Proposed tension model

In defining an average stress-strain formulation to model tension softening behavior, the model must be a function of a certain representative length of material L_r in which a crack is assumed to be distributed uniformly. The representative length is primarily dependent on the crack spacing, and can be estimated based on the structure geometry and reinforcement details. For reinforced concrete thick-shell structures critical in shear, the representative length L_r can be taken as

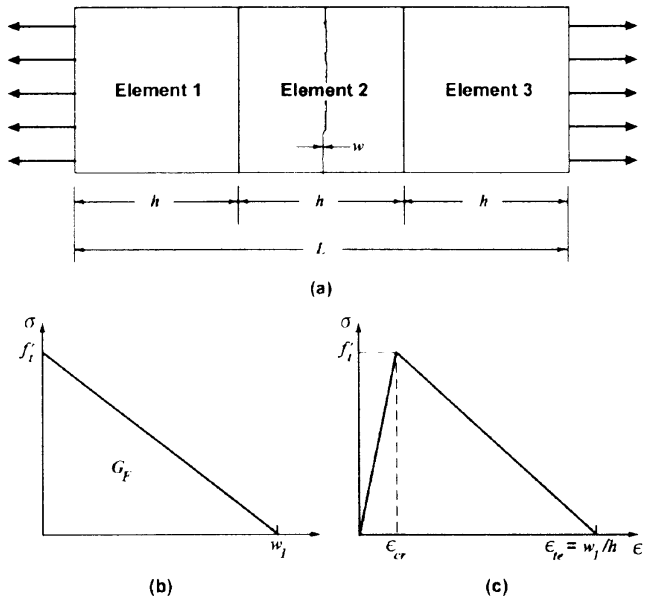

Fig. 3—Tension softening in concrete: (a) concrete element subjected to tension; (b) stress-crack formulation approach; and (c) stress-strain formulation approach.

$$L_r = d/2 \tag{1}$$

where d is the depth to the centroid of the tension reinforcement measured from the compressive face of the shell section. Hence, the proposed formulation for the basic tension softening stress f_{c1b} is as follows

$$f_{c1b} = \begin{cases} E_c \cdot \varepsilon_1, & \le \varepsilon_1 \le \varepsilon_{cr} \\ \dfrac{f_c'}{1 + \sqrt{k_s(\varepsilon_1 - \varepsilon_{cr})}}, & \varepsilon_{cr} \le \varepsilon_1 < \varepsilon_{ch} \\ \dfrac{(\varepsilon_{te} - \varepsilon_1)}{(\varepsilon_{te} - \varepsilon_{ch})} \cdot f_{ch}, & \varepsilon_{ch} \le \varepsilon_1 < \varepsilon_{te} \\ 0, & \varepsilon_{te} < \varepsilon_1 \end{cases} \tag{2}$$

where

$$\varepsilon_{ch} = \frac{2G_f}{L_r \cdot f_t'} \tag{3}$$

$$\varepsilon_{te} = 5\varepsilon_{ch} \tag{4}$$

$$f_{ch} = \frac{f_t'}{1 + \sqrt{k_s(\varepsilon_{ch} - \varepsilon_{cr})}} \tag{5}$$

The tension softening coefficient k_s is determined from the following condition

$$\int_0^\infty f_{c1b}\, d\varepsilon = \frac{G_f}{L_f} \tag{6}$$

The concrete tensile strength f_t' and cracking strain ε_{cr} can be established as follows

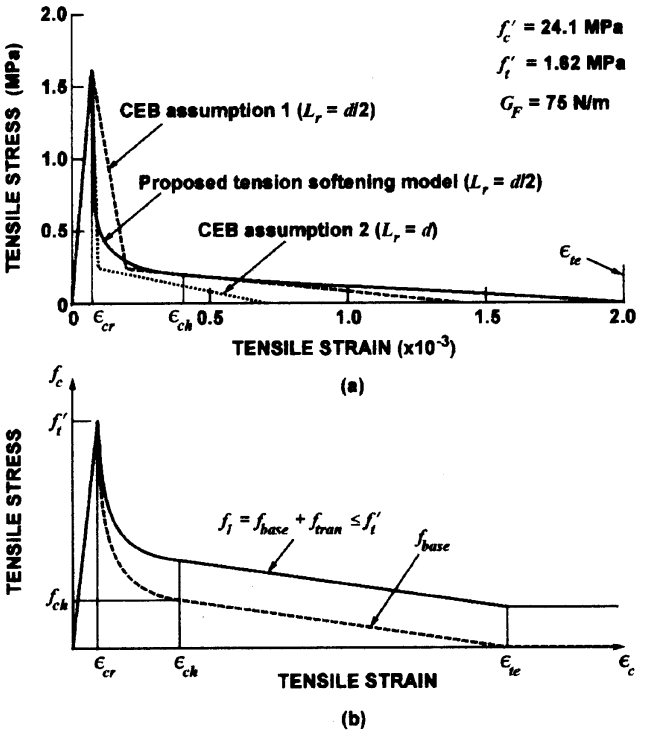

Fig. 4—Proposed concrete tension model: (a) base model compared to CEB formulations; and (b) total stress.

$$f_t' = 0.65(f_c')^{0.33} \tag{7}$$

and

$$\varepsilon_{cr} = \frac{f_t'}{E_c} \tag{8}$$

where E_c is the initial tangent stiffness of the concrete and f_c' is the concrete compressive strength.

Shown in Fig. 4 is the proposed formulation together with the tension-softening model of the CEB-FIP Model Code (1990). When a representative length of d is used in the CEB model, the tension-softening response exhibits a sharp initial drop at cracking, and a rapid decline thereafter. It was found that the initial large drop in tensile stress is important in accurately representing behavior at stages of loading prior to initiation of shear failure. Also shown is the CEB model based on a representative length of $d/2$; herein, the initial decline is less abrupt, and the decay thereafter is more gradual. The gradual decay in tension stress portrayed in the second variation of the CEB model was found to better predict the response after the development of shear cracking up to failure. The proposed model combines these two important features: a large initial drop in stress followed by a gradual decay thereafter.

In cases where transverse (shear) reinforcement is present, tension stiffening mechanisms add to the tensile stress being developed. In a typical layered thick-shell formulation, the stress-strain relationship of the transverse reinforcement is defined as elastic-plastic; that is, no strain hardening is considered. In reality, transverse reinforcement has not only yielded but also hardened in the vicinity of cracks, even though the average strain may be significantly less than the yield strain. As a consequence, tensile stresses in the concrete can continue to be transmitted across cracks after yielding of the transverse reinforcement. To account for these tension-stiffening effects in the proposed formulation, an additional tension term is defined as

$$f_{c1t} = \alpha \cdot \rho_t \cdot (f_u - f_y) \cdot \cos^2\theta_n \tag{9}$$

where α is the effective hardening coefficient, taken as 0.80; ρ_t is the transverse reinforcement ratio; f_u is the ultimate strength of the transverse steel; f_y is the yield strength of the transverse steel; and θ_n is the angle of the normal to the crack with respect to the transverse reinforcement direction. If the transverse reinforcement has not yielded, the average stress f_s is substituted for the yield stress f_y in Eq. (9).

The total tension in the concrete is obtained by adding the base tension softening stress to the concrete tensile stress arising from the strain hardening effect; that is

$$f_{c1} = f_{c1b} + f_{c1t} \tag{10}$$

Note that the previous formulation applies to concrete outside the tension-stiffening zones of the in-plane reinforcement. For concrete within the tension-stiffening zones, the formulations previously proposed in the MCFT apply; that is

$$f_{c1} = \frac{f_t'}{1 + \sqrt{c_t \varepsilon_1}} \tag{11}$$

The tension stiffening coefficient c_t depends on a number of factors including specimen size and reinforcing bar diameters; however, $c_t = 500$ can be taken as an average value. All reinforcement contributes to tension-stiffening stresses, including transverse reinforcement. The contributions, however, are assumed to diminish to zero as the reinforcement yields across cracks (refer to Vecchio and Collins 1986).

TRANSVERSE SHEAR TESTS

The analytical procedure was previously corroborated against test results from simple shell element panels (Polak and Vecchio 1994) and from slab specimens subjected to various transverse loading conditions (Vecchio et al. 1993; Vecchio and Tata 1999). While the correlation between calculated and observed behavior was typically very good, these specimens were not generally critical in shear. A more stringent test of the accuracy of the proposed formulation in modeling transverse shear in thick-shell elements can be obtained by modeling shear-critical beam specimens.

The series of 12 beams tested by Bresler and Scordelis (1963) provides a suitable range of conditions. The beams were of various lengths, simply supported and subjected to a center-point loading; the shear span-depth ratios ranged between 4 and 7. Three of the beams contained no shear reinforcement; the others contained shear reinforcement ratios ranging from 0.1 to 0.2%. Heavy amounts of longitudinal reinforcement were provided to mitigate against flexural failure. Full specimen details are provided by Yamamoto (1999).

The three beams without shear reinforcement (OA-1, OA-2, and OA-3) were found to experience diagonal tension shear failure shortly after the formation of the first (critical) diag-

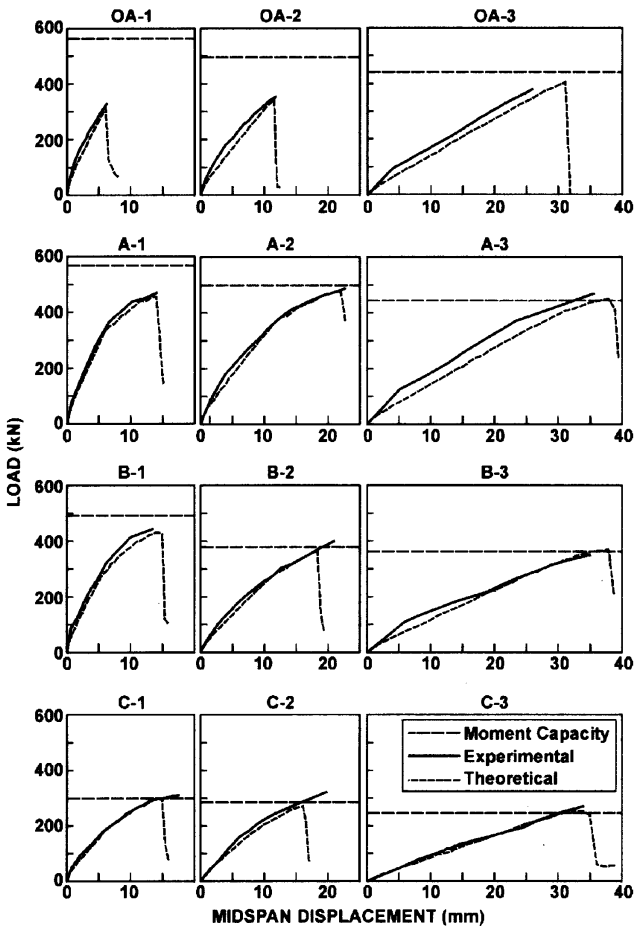

Fig. 5—Comparison of observed and calculated load-deflection responses for Bresler-Scordelis beams.

onal shear crack. Six of the beams (A-1, A-2, B-1, B-2, C-1, and C-2) experienced what will be categorized as a shear-compression failure. Herein, flexural cracks were first observed, followed by the formation of shears cracks, ending with a failure involving shear/crushing of concrete in the compression zone. The remaining three beams (A-3, B-3, and C-3), being long-span and heavily reinforced in flexure, experienced flexure-compression failures.

The beams were modeled for analysis using shell elements oriented transverse to the load direction (that is, so that the shear forces were acting out-of-plane). Due to the symmetrical nature of the beam details and loading conditions, only 1/2 of the beams were modeled. A 7 x 1 element mesh was used for the 3660 mm length beams; an 8 x 1 mesh for the 4570 mm beams; and a 12 x 1 mesh for the 6400 mm beams. Each element employed 12 equal-thickness layers through the 550 mm beam depth. Loading was represented as an imposed displacement at the beam midspan. Increments of nodal displacement of 0.5 mm were used for the short and middle length beams, and 1.0 mm for the longer beams.

The calculated load-deflection response for each of the 12 beams is compared with the experimental results in Fig. 5. In all cases, there is good agreement in terms of predicted strength, stiffness, and ductility. Particularly noteworthy is the strong correlation obtained for the beams containing no shear reinforcement and failing in a shear critical mode (that is, Beams OA-1, OA-2, and OA-3). In these beams, the tension-stiffening zone extended only up to approximately the mid-depth of the cross section, and hence, tension-softening

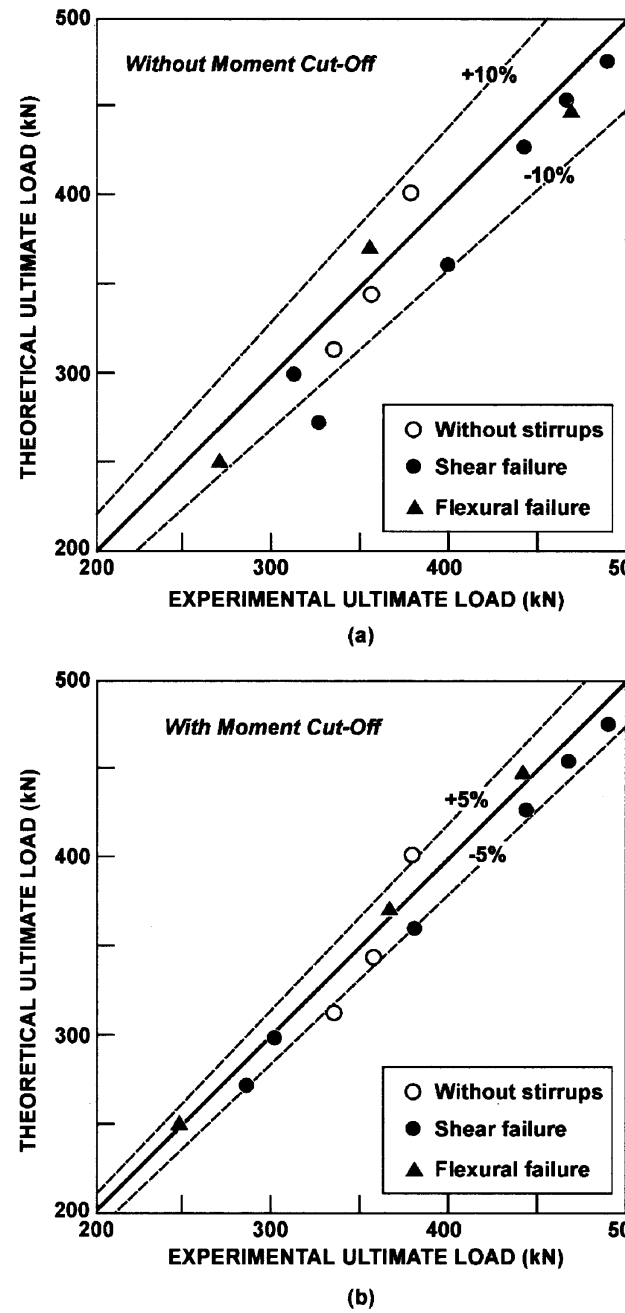

Fig. 6—Comparison of experimental and theoretical load capacities for Bresler-Scordelis beams: (a) without flexural limit cutoff; and (b) with flexural limit cutoff.

contributions to response were critical. Omitting the tension-softening contribution results in significantly underestimated strengths for the OA set of beams. Figure 6(a) compares the ratio of experimental-to-calculated shear strength for the 12 beams; this ratio was found to have a mean of 0.96 and a coefficient of variation (COV) of 6.2%. Note, however, that six of the beams achieved test loads exceeding their theoretical pure moment capacity. If the experimental loads are cut off at the moment capacities, then the ratio of observed-to-predicted strength improves to a mean of 0.99 and a COV of 3.8% (Fig. 6(b)). Since the behavior of these beams is highly dependent on the accurate representation of concrete tensile stresses, they provide a valuable corroboration of the proposed concrete tension model.

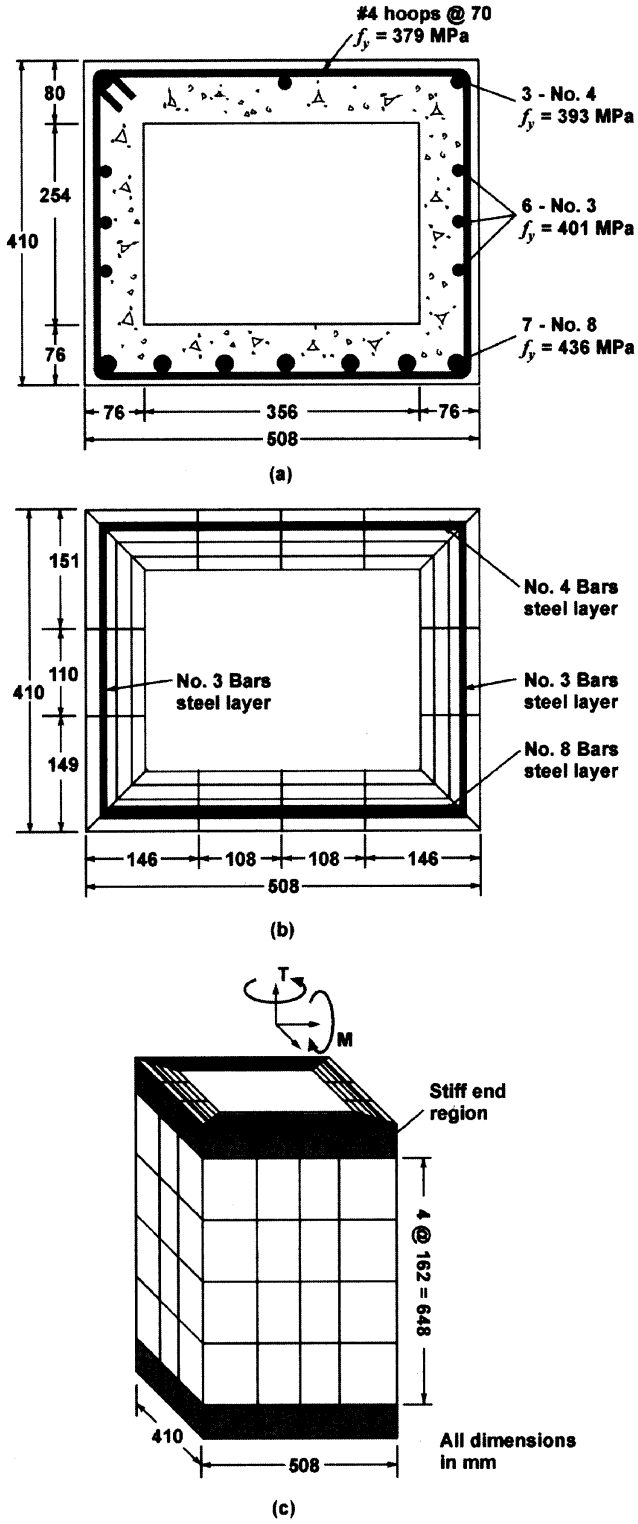

Fig. 7—Details of Onsongo torsion beams: (a) cross section details; (b) finite element mesh; and (c) layer definition.

TORSIONAL SHEAR TESTS

In addition to transverse shear, concrete thick shell structures can be subjected to significant levels of torsional shear and in-plane shear stresses. Beam tests conducted by Onsongo (1978) provide a useful calibration of the model's accuracy in this regard. Onsongo tested two series of hollow concrete beams: the TBO series and the TBU series. In each, five hollow concrete beams were subjected to a uniform

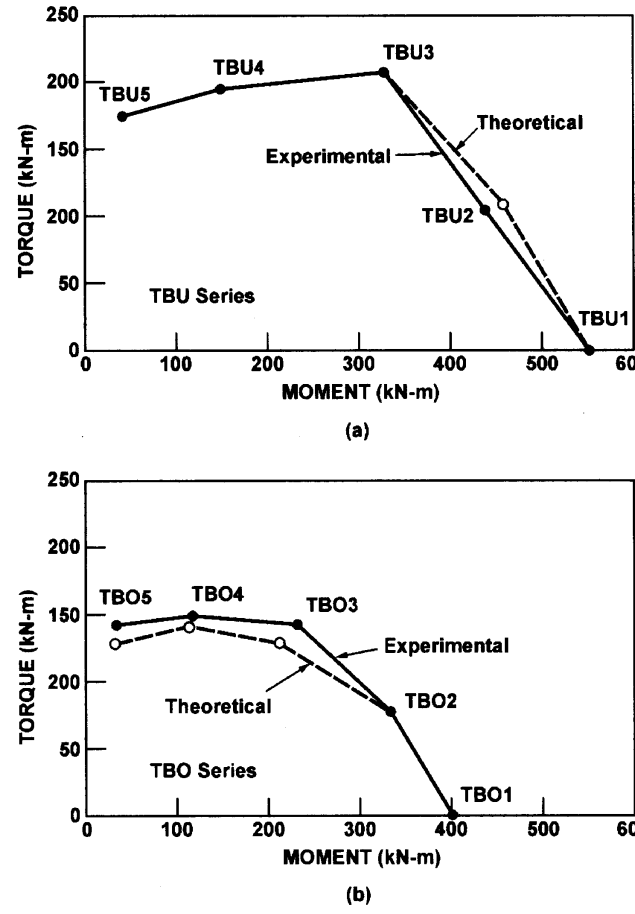

Fig. 8—Flexure-torsion strength interaction diagrams for Onsongo beams: (a) TBU Series beams; and (b) TBO Series beams.

bending moment and torque along their lengths and loaded to failure. All beams had essentially the same reinforcement conditions, but the concrete strengths between the two series differed. The TBO series beams employed lower concrete strengths and were characterized as over-reinforced, whereas the TBU series beams contained higher-strength concrete, and hence, were under-reinforced. In each series, the test beams varied in the ratio of moment to torque applied, ranging from flexure-dominant to torsion-dominant. The beam section and reinforcement details are shown in Fig. 7(a); again, full details are provided by Yamamoto (1999).

Since the test specimens were subjected to constant moment and torque along their lengths, only a portion of the specimens were modeled. Figure 7(b) and (c) show the finite element model and concrete section details used. A 648 mm length of beam was modeled with a mesh of 56 elements, each of which employed four layers through their thickness. To safely apply forces to the structure, 14 subsidiary elements were added at each end of the model; these end-zone elements were defined with stiff elastic material properties and only one layer through the thickness. Bending and torsional moments were applied as nodal forces at the member ends. Approximately 20 to 25 equal-increment load stages were used to load the beams to failure.

Fig. 8 contains flexure-torsion interaction diagrams for the two series of beams, comparing the experimental and calculated strengths. Shown in Fig. 9 are the torque-twist and torque-hoop strain response curves for specimens TBO3 and

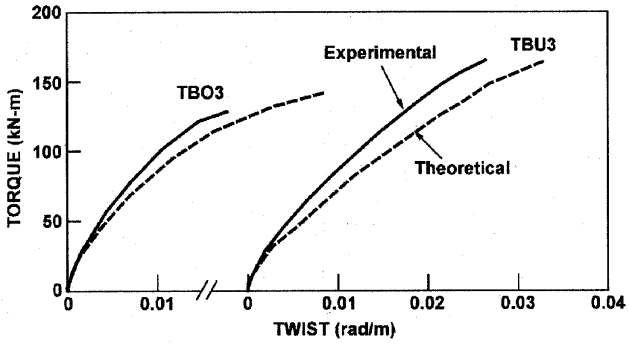

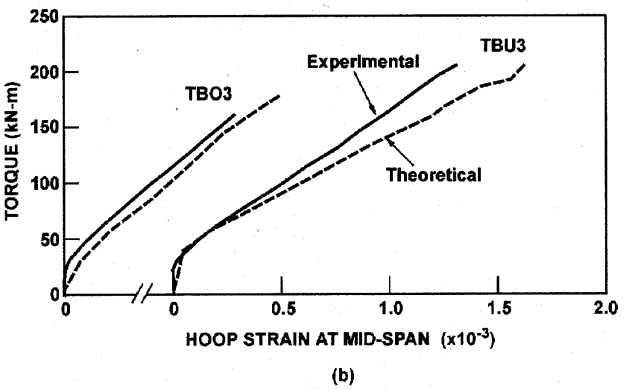

Fig. 9—Comparison of experimental and theoretical responses for typical Onsongo beams: (a) torque-twist response; and (b) torque-hoop strain response.

TBU3, being representative of the level of correlation obtained. In general, the analytical results agree reasonably well with the experimentally observed behavior for both the TBO and TBU series in facets of response including strength, stiffness, ductility, and failure mode. The ratio of experimental-to-calculated ultimate load for the two series combined had a mean of 1.00 and a COV of 6.9%.

It should be noted that all of the beams sustained a shear/crushing failure of the concrete, with most prior to yielding of either the longitudinal or hoop reinforcement. This being the case, the inclusion of adequate models for representing concrete tension-stiffening, concrete tension-softening, and concrete compression-softening mechanisms was indispensable in accurately capturing the postcracking response. Spalling was observed in some of the specimens subjected to high torque, but was not accounted for in the analytical model. The influence of spalling was minor since the concrete cover used in these specimens was uncommonly thin.

CONDEEP CELL MODEL

The test specimens examined to this point involved well-controlled, statically determinate load conditions. In complex shell structures, the variation of out-of-plane shears and moments is generally statically indeterminate, rapidly changing, and concentrated at joints and transition points. The modeling of strength and behavior in such structures is considerably more challenging. To examine the accuracy of the proposed formulation in such situations, a large-scale hydrostatically loaded cell structure was modeled.

The test conducted by Helmy (1998) involved a 1:13 scale model of a typical storage cell in an early Condeep structure (a concrete gravity-base offshore structure) shown in Fig. 10(a).

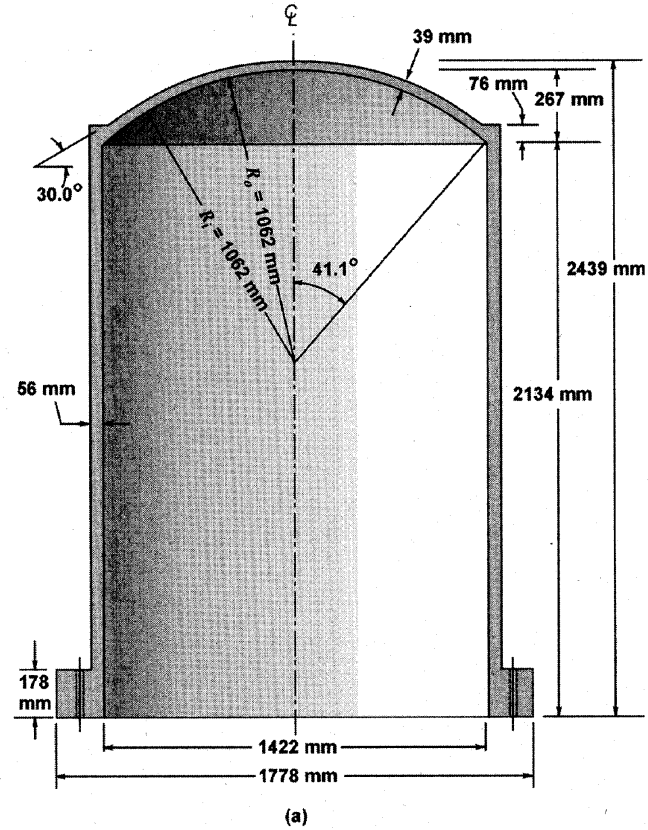

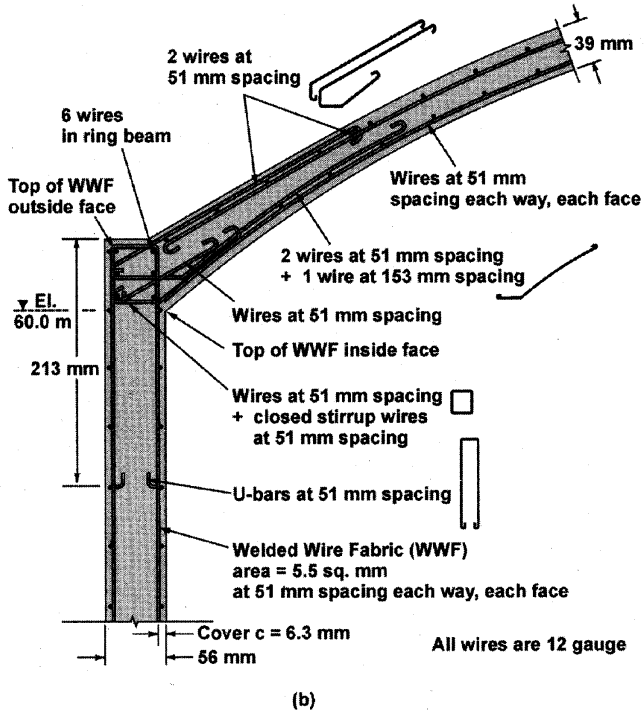

Fig. 10—Details of Condeep model tested by Helmy: (a) overall geometry; and (b) reinforcement details.

The specific detail modeled by the test structure was the junction between the upper dome and the cylindrical cell wall of the storage cell. The reinforcement used in the construction of the model was 12-gage galvanized steel wire, provided in the form of welded wire fabric for the cylinder walls, and as individual wires for the dome and ring beam areas. Figure 10(b) shows the reinforcement details near the

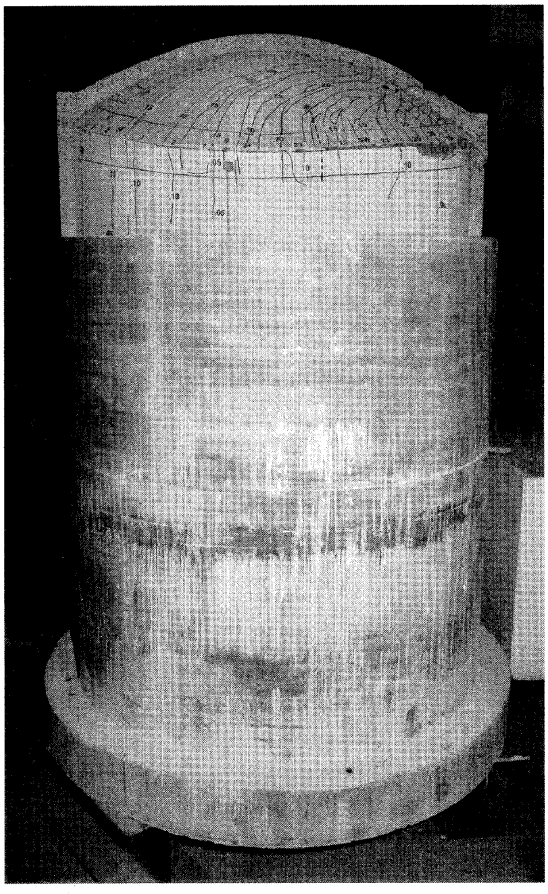

(a)

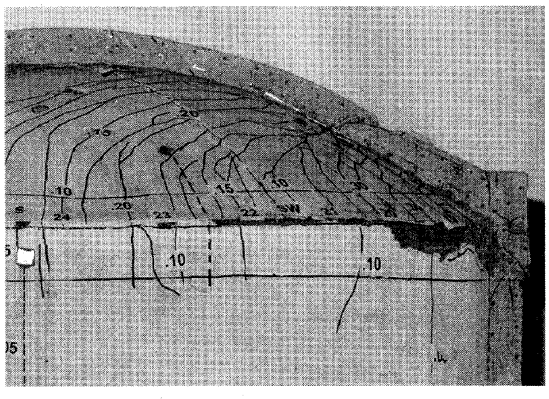

(b)

Fig. 11—(a) Photo of shear failure below ring-beam of offshore model; and (b) cut-away view.

dome-wall junction. Note that no shear reinforcement is explicitly provided. A high-strength concrete of 75 MPa strength, with a maximum coarse aggregate of 4.5 mm crushed limestone, was used in casting the specimen. To simulate prestressing in the ring-beam, a 7 mm diameter high-strength prestressing wire was placed circumferentially at the intersection of the upper dome and cell wall.

The model was subjected to external hydrostatic pressure. Water pressure was gradually increased until the specimen failed (severe loss of containment) at an applied pressure of 1.48 MPa. At this ultimate load, a sudden shear failure occurred across the cell wall just below the wall-dome junction. A cut-away view of the failure zone is seen in Fig. 11.

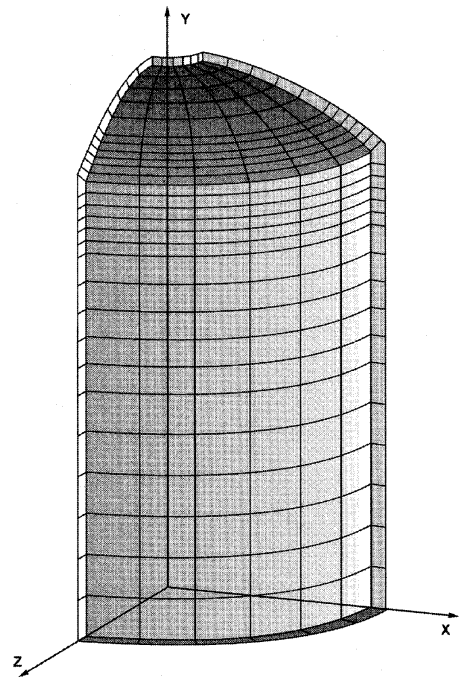

Fig. 12—Finite element mesh used to model Helmy structure.

The finite element mesh used to model a quarter-section of the test specimen is shown in Fig. 12 (note that an axisymmetrical element was not available in the finite element program used). A total of 162 quadrilateral elements were used in the modeling. Geometry constraints required that a 94 mm radius hole be left at the apex of the dome; it is believed that this had some influence on the predicted deflections at the top of the dome but did not otherwise significantly influence the calculated strength and response of the structure. An initial hydrostatic pressure of 1.01 MPa was applied to the vertical outside face of the ring-beam elements only; this initial load was used to represent the effects of prestressing of the ring-beam. Additional water pressure loads were then applied to all external surfaces of the model, and increased in 0.05 MPa increments until the maximum load capacity of the structure was exceeded.

Convergence was quick and stable to loads of about 1.40 MPa pressure, indicating an essentially uncracked response. At 1.45 MPa, a sudden and brittle shear failure occurred in the elements immediately below the ring-beam; this was in excellent agreement with the ultimate load and failure mode observed experimentally. Shown in Fig. 13(a) and (b) are the observed and calculated load-deflection responses at the quarter-points of the dome and at the midheight of the cylinder wall, respectively. While some disparity can be seen, the correlation between predicted and observed response is reasonably good. It is presumed that the modeling detail of the dome had some influence on the accuracy of the dome deflections. The accurate simulation of the failure of the cell wall in transverse shear, particularly since the wall contained no shear reinforcement, again provides valuable corroboration of the concrete tension model.

CONCLUSIONS

A concrete tension-softening model was developed, using an average strain approach, in a form substantially different from that commonly used for tension softening. Most formulations

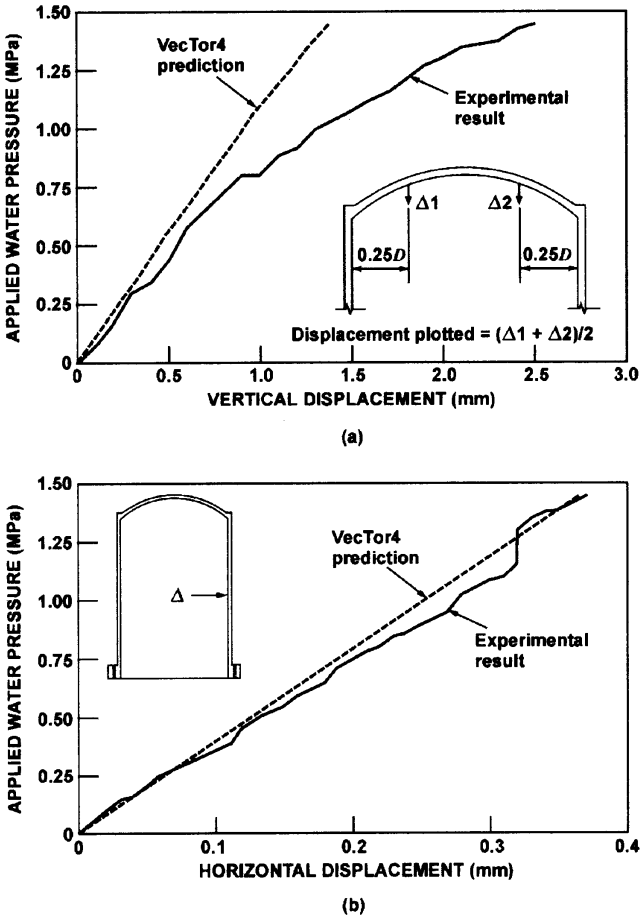

Fig. 13—Comparison of theoretical and experimental load-deflection response for Helmy structure: (a) vertical displacements of dome; and (b) radial displacement of cell wall at midheight.

will use a smeared cracking assumption and principles of fracture mechanics to pursue the modeling of the discretized governing crack. The formulation proposed herein, although also utilizing the concepts of smeared cracking and fracture energy, describes the average behavior of structural elements. The average strain approach is favored herein because it is consistent with the formulations of the MCFT and other similar smeared rotating crack models, and it can easily be incorporated into general nonlinear finite element formulations.

The proposed tension model was implemented in program VecTor4, a nonlinear finite element analysis program for concrete thick-shell structures. The analysis program was then tested against the results of three series of experiments. In the modeling of beams critical in transverse shear, the formulation was able to accurately portray all aspects of response including strength, stiffness, ductility, and failure mode. Governing failure mechanisms ranging from diagonal-tension failure to shear-compression failure and flexure-compression failure were equally well-represented. In the analysis of beam elements critical in torsional shear, similarly good correlation was found. Lastly, the analysis program was used to model a large-scale domed cylindrical structure subjected to hydrostatic pressure and failing in transverse shear. The strength and failure mode were well represented.

A tension-softening model is indispensable in accurately representing the behavior of concrete structures containing large areas of plain (unreinforced) concrete. The consideration of concrete tension stiffening, within an appropriate effectiveness zone, and concrete compression softening are also essential in the analysis of reinforced concrete shell structures where in-plane or out-of-plane shear is a concern. The formulations proposed herein appear to provide good correlations with observed response, and are amenable to implementation in finite element models using layered elements.

NOTATION

c_t = tension stiffening coefficient
d = depth to centroid of longitudinal reinforcement
E_c = initial tangent modulus of concrete
f_c' = compressive strength of concrete
f_{c1} = average principal tensile stress in concrete
f_t' = tensile strength of concrete
f_u = ultimate stress of reinforcement
f_y = yield stress of reinforcement
G_f = fracture energy
k_s = tension softening coefficient
L_r = representative length
α = effective hardening coefficient
ε_{c1} = average principal tensile strain in concrete
ε_{cr} = concrete cracking strain
ρ_t = transverse reinforcement ratio
θ_n = inclination of crack with respect to transverse reinforcement

REFERENCES

An, X.; Maekawa, K.; and Okamura, H., 1997, "Numerical Simulation of Size Effect in Shear Strength of RC Beams," *Journal of Materials Concrete Structures*, JSCE, V. 35, No. 564, pp. 297-316.

ASCE, 1993, "Finite Element Analysis of Reinforced Concrete II," *Proceedings International Workshop*, ASCE, New York, 717 pp.

Bresler, B., and Scordelis, A. C., 1963, "Shear Strength of Reinforced Concrete Beams," ACI JOURNAL, *Proceedings* V. 60, No. 1, Jan., pp. 51-74.

CEB, 1990, "CEB-FIP Model Code 1990," *Bulletin d'Information du Comite Euro-International du Beton*, 437 pp.

Cervera, M.; Hinton, E.; and Hassan, O., 1987, "Nonlinear Analysis of Reinforced Concrete Plate and Shell Structures Using 20-Noded Isoparametric Brick Elements," *Computers and Structures*, V. 25, No. 6, pp. 845-869.

Darwin, D., 1999, "Fracture Mechanics," *Memorandum*, ACI Committee on Shear and Torsion, Mar. (unpublished)

Di, S., and Cheung, Y. K., 1993, "Nonlinear Analysis of RC Shell Structures Using Laminated Element I," *ASCE Journal of Structural Engineering*, V. 119, No. 7, pp. 2059-2073.

Hand, F. R.; Pecknold, D. A.; and Schnobrich, W. C., 1977, "Nonlinear Layered Analysis of RC Plates and Shells," *ASCE Journal of the Structural Division*, V. 99, No. ST7, pp. 1491-1505.

Harmon, T. G., and Zhangyuan, N., 1989, "Shear Strength of Reinforced Concrete Plates and Shells Determined by Finite Element Analysis Using Layered Elements," *ASCE Journal of Structural Engineering*, V. 115, No. 5, pp. 1141-1157.

Helmy, A. I. I., 1998, "Behavior of Offshore Reinforced Concrete Structures under Hydrostatic Loading," PhD thesis, Department of Civil Engineering, University of Toronto, 217 pp.

Hu, H. T., and Schnobrich, W. C., 1991, "Nonlinear Finite Element Analysis of Reinforced Concrete Plates and Shells under Monotonic Loading," *Computers and Structures*, V. 38, No. 5/6, pp. 637-651.

Jofriet, J. C., and McNeice, G. M., 1971, "Finite Element Analysis of Reinforced Concrete Slabs," *ASCE Journal of the Structural Division*, V. 97, No. ST3, pp. 785-806.

Mihashi, H.; Okamura, H.; and Bažant, Z. P., 1993, "Numerical Simulation of Size Effect in Shear Strength of RC Beams," *Proceedings*, Japan Concrete Institute International Workshop, JCI, Sendai, Japan, 552 pp.

Onsongo, W. M., 1978, "The Diagonal Compression Field Theory for Reinforced Concrete Beams Subjected to Combined Torsion, Flexure and Axial Load," PhD thesis, Department of Civil Engineering, University of Toronto, 246 pp.

Polak, M. A., 1998, "Modeling Punching Shear of Reinforced Concrete Slabs Using Layered Finite Elements," *ACI Structural Journal*, V. 95, No. 1, Jan.-Feb., pp. 1-10.

Polak, M. A., and Vecchio, F. J., 1994, "Reinforced Concrete Shell Elements Subjected to Bending and Membrane Loads," *ACI Structural Journal*, V. 91, No. 2, Mar.-Apr., pp. 261-268.

Polak, M. A., and Vecchio, F. J., 1993, "Nonlinear Analysis of Reinforced Concrete Shells," *ASCE Journal of Structural Engineering*, V. 119, No. 12, pp. 3439-3461.

Scordelis, A. C., and Chan, E. C., 1987, "Nonlinear Analysis of Reinforced Concrete Shells," *Computer Applications in Concrete Technology*, SP-98, American Concrete Institute, Farmington Hills, Mich., pp. 25-57.

Vecchio, F. J.; Agostino, N.; and Angelakos, B., 1993, "Reinforced Concrete Slabs Subjected to Thermal Loads," *Canadian Journal of Civil Engineering*, V. 21, No. 5, pp. 741-753.

Vecchio, F. J., and Collins, M. P., 1986, "The Modified Compression Field Theory for Reinforced Concrete Elements Subjected to Shear," *ACI Structural Journal*, V. 83, No. 6, pp. 925-933.

Vecchio, F. J., and Tata, M., 1999, "Approximate Analyses of Reinforced Concrete Slabs," *Structural Engineering and Mechanics*, V. 8, No. 1, pp. 1-18.

Yamamoto, T., 1999, "Nonlinear Finite Element Analysis of Transverse Shear and Torsional Problems in Reinforced Concrete Shells," MASc thesis, Department of Civil Engineering, University of Toronto, 112 pp.